Nonlinear Dyn
https://doi.org/10.1007/s11071-020-05632-4

ORIGINAL PAPER

Stationary response probability density of nonlinear random vibrating systems: a data-driven method

Yanping Tian · Yong Wang · Hanqing Jiang · Zhilong Huang · Isaac Elishakoff · Guoqiang Cai

Received: 8 November 2019 / Accepted: 5 April 2020

Abstract A data-driven method is established to derive the (approximately) analytical expression of the stationary response probability density of nonlinear random vibrating system, which explicitly includes system features and intensity of excitation. The stationary response probability density is first assumed as an exponential form by using the principle of maximum entropy. Through the rule of dimensional consistency, the power of exponential function is expressed as a linear combination of a set of nondimensional parameter clusters which are constituted by system features, intensity of excitation, and state variables. By comparing the power of exponential function with the approximate logarithm probability density evaluated from simulated data statistically, the determination of unknown coefficients comes down to the solution of (overdetermined) simultaneous linear algebraic equations. The data-driven method rediscovers the exact stationary response probability density of random-excited Duffing oscillator and derives an approximately analytical expression of stationary response probability density of van der Pol system from the simulated data of six cases with different values of system features and intensity of excitation. This data-driven method is a unique method which can explicitly include the information of system and excitation in the analytical expression of stationary response probability density. It avoids the solution of simultaneous nonlinear algebraic equations encountered in the maximum entropy method and closure methods and, in the meanwhile, avoids the sophisticated selection of weighting functions in closure methods.

Keywords Stationary response probability density · Nonlinear random vibrating system · Data-driven method · Dimensional analysis · Simulated data

Y. Tian
College of Mechanical Engineering, Hangzhou Dianzi University, Hangzhou 310018, China

Y. Wang (✉) · Z. Huang
Department of Engineering Mechanics, Zhejiang University, Hangzhou 310027, China
e-mail: ypwang@zju.edu.cn

H. Jiang
School for Engineering of Matter, Transport and Energy, Arizona State University, Tempe, AZ 85287, USA

I. Elishakoff · G. Cai
Department of Ocean and Mechanical Engineering, Florida Atlantic University, Boca Raton, FL 33431, USA

1 Introduction

Nonlinear random vibration phenomena are ubiquitous in the fields of mechanical engineering, civil engineering, and other technologies, such as the responses of a tower-shaped structure subjected to

Published online: 05 May 2020

severe seismic excitations, a moving vehicle excited by real rough road surfaces, and an aerospace structure acted by severe atmospheric turbulence [1, 2]. The exact prediction of the response probability density is of great significance to evaluate the operating performance, stability and reliability, and then guide the design for reliability [3, 4]. The nonlinearity can arise from various sources: the material nonlinearity (such as the nonlinear stress–strain relation including a hysteretic loop), the geometric nonlinearity (such as the nonlinear strain–displacement relation due to large deformation and the nonlinear damping with displacement-dependent damping coefficient), and the topological nonlinearity (such as physical barriers limiting the motion) [5]. Also, various random excitations exhibit quite different properties in the aspects of probability and correlation. Due to the nonlinearity of systems themselves and the uncertainty of random excitations, it is quite difficult to exactly predict the probability densities of transient/stationary responses.

Nonlinear random vibrating systems are mathematically described by simultaneous second-order nonlinear stochastic differential equations (NSDEs) [3, 4]. The representative methods establishing the transient/stationary probability densities *directly* from the NSDEs are the Monte Carlo simulation and the maximum entropy method. The Monte Carlo simulation statistically evaluates the approximate probability densities of state variables at discrete grids from the discrete simulated data of plenty of samples [6]. The maximum entropy method seeks the approximate probability density function maximizing the Shannon informational entropy under the constraints of various order moments and normalization condition [7–9], in which the various order moments are determined by the moment equations derived from the NSDEs, and the functional extreme value problem with constraints is solved by introducing Lagrangian multipliers. The probability density is expressed as an exponential function of the summation of Lagrangian multipliers multiplying functions of state variables; then, the Lagrangian multipliers are determined by solving a set of nonlinear differential equations (for the transient cases) or nonlinear algebraic equations (for the stationary cases).

For the random vibrating systems with Gaussian white noise or filtered white noise excitation, the response probability density function satisfies the Chapman–Kolmogorov–Smoluwski (CKS) equation and the Fokker–Plank–Kolmogorov (FPK) equation [3, 4]. The CKS equation is an integral equation governing the transition probability density, while the FPK equation is a parabolic partial differential equation with first-order derivative to time and second-order derivatives to state variables. Almost all the existing literatures derive the response probability densities of nonlinear random systems by solving the associated FPK equation, analytically or numerically. Only for a few simple and low-dimensional nonlinear systems, the exact stationary probability density is derived by using the detailed balance or generalized stationary potential methods [3, 4, 10]. Even for these systems with exact stationary solutions, there always exist some solvability conditions which are too strict to be satisfied in actual situations. Thus, many purely numerical procedures have been adopted, such as the finite difference method, finite element method [11, 12], generalized cell mapping technique [13, 14] and path integration method [15–17]. These purely numerical procedures are versatile, while only give the discrete values in preset grids.

A lot of literatures devote the semianalytical procedures to solve the FPK equation, such as the equivalent methods (including statistical linearization and equivalent nonlinear system [4, 18]), the closure methods (including Gaussian [19], non-Gaussian [20] and exponential [21–23], and its variants [24–26]). The equivalent methods first preselect a special system family with exact solution and then determine the optimal approximation of the nonlinear system in a certain statistical sense. The application of equivalent linearization method is confined to weakly nonlinear systems, while the application of equivalent nonlinear system method is limited by the preselection of system family. The Gaussian closure technique is equivalent to the statistical linearization method for the systems with Gaussian white noise excitations and only effective for the systems with weak nonlinearity. The non-Gaussian closure technique expands the probability density as various series and then determines the undetermined coefficients of the series. This method, however, cannot guarantee the nonnegative property of the probability density. The exponential closure technique assumes the probability density can be approximated by an exponential function of polynomial in state variables and then determines the undetermined coefficients by (iterative) weighted residual method. This method guarantees the

nonnegative property of the probability density, while the simultaneous nonlinear differential or algebraic equations must be solved, and the prediction accuracy is strongly dependent on the selection of weighting functions.

The existing methods for determining the response probability densities of nonlinear random vibrating systems are summarized in Fig. 1. The methods starting from the NSDEs do not limited by the styles of random excitations, while those starting from the FPK equation are confined to the (filtered) Gaussian white noise excitations. Furthermore, all the existing methods possess some disadvantages. For instance, the purely numerical methods only give the discrete values in preset grids. The equivalent methods are limited by the strength of nonlinearity and the scarcity of system families with exact solutions. The maximum entropy methods and the closure methods come down to the solution of a set of simultaneous nonlinear differential or algebraic equations. Furthermore, the accuracy of the closure methods is strongly dependent on the selection of weighting functions. Thus, *it is deserved to develop a new method to derive the (approximately) analytical expression of transient/stationary probability density directly from the NSDEs, without involving the solution of simultaneous nonlinear differential/algebraic equations and the preselection of weighting functions.*

This manuscript devotes to establish a data-driven method to derive the (approximately) analytical expression of stationary response probability density of nonlinear random vibrating systems. The method starts from the discrete simulated data and comes down to the solution of a set of (overdetermined) linear algebraic equations. The manuscript is organized as follows: Sect. 2 states the whole process of the methodology, including the exponential assumption of stationary response probability density, the determination of possible parameter clusters, the optimization criterion, and the optimization algorithm; two typical examples, i.e., Duffing oscillator (with exact solution) and van der Pol system (without exact solution), are investigated in Sects. 3 and 4 to illustrate the application and efficacy of the data-driven method; Sect. 5 concludes this work and gives some discussions.

2 Whole process of data-driven method

This section demonstrates the whole process of the data-driven method step by step. This method starts from the simulated data of NSDEs; thus, there is no limitation on the styles of random excitations. For simplicity, the random excitations are confined to Gaussian white noises in what follows.

2.1 Mathematical description and data acquisition of nonlinear random vibrating systems

A nonlinear random vibrating system excited by Gaussian white noises can be described by the stochastic differential equations,

$$\mathbf{\Gamma}(\ddot{\mathbf{q}}, \dot{\mathbf{q}}, \mathbf{q}, \mathbf{s}, \mathbf{W}) = 0 \tag{1}$$

in which $\mathbf{q} = \{q_1, q_2 \ldots, q_n\}$ denotes (generalized) displacements and the over dot means the derivative with respect to time t. $\mathbf{s} = \{s_1, s_2, \ldots s_l\}$ is system

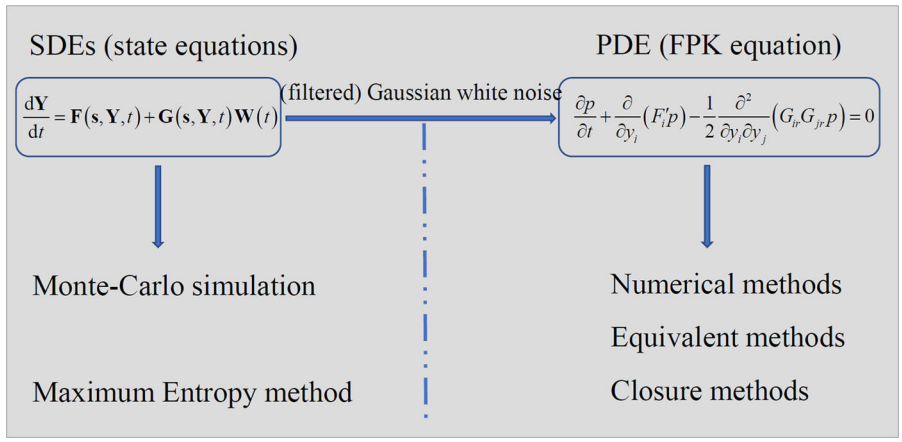

Fig. 1 Existing methods for predicting the response probability density of random-excited systems

feature, such as mass, stiffness and damping. $\mathbf{W} = \{W_1, W_2 \ldots, W_m\}$ is a Gaussian white noise vector with zero mean and correlation function $E[\mathbf{W}(t)\mathbf{W}(t+\tau)] = 2\mathbf{D}\delta(\tau)$, in which the intensity $2\mathbf{D} = \left[2D_{ij}\right]_{m\times m}$ is symmetric and generally nondiagonal. The output (i.e., generalized displacement $\mathbf{q}$) depends on the system itself (i.e., system feature $\mathbf{s}$) and the input (i.e., random excitation $\mathbf{W}$).

Regardless of the complexity induced by high dimension, strong nonlinearity, and/or uncertainty of random excitations, the approximate values of stationary response probability density at preset grids can be evaluated from the simulated data statistically, i.e., record the simulated data, statistically calculate the probability in discrete domains, and evaluate the approximate values of probability density at preset grids. The *approximate* stationary probability density at preset grids $\left(\mathbf{q}_i, \dot{\mathbf{q}}_j\right)$ is denoted as $\hat{p}_s(\mathbf{s}, \mathbf{D}, \mathbf{q}, \dot{\mathbf{q}})$, which depends on system feature $\mathbf{s}$ and intensity of excitation $2\mathbf{D}$. This method starts from the simulated data (maybe the simulated data from the same system with different values of system feature and excitation intensity), statistically evaluates the approximate stationary probability density at preset grids, and derives the explicit relation between the stationary probability density, system feature, intensity of excitation, and state variables.

2.2 Exponential assumption of stationary probability density

Referring to the maximum entropy method and exponential closure method, the stationary joint probability density of state variables of nonlinear random vibrating systems can be expressed as the following exponential form,

$$p_s(\mathbf{s}, \mathbf{D}, \mathbf{q}, \dot{\mathbf{q}}) = \exp[f(\mathbf{s}, \mathbf{D}, \mathbf{q}, \dot{\mathbf{q}})] \tag{2}$$

in which the power of exponential function $f(\mathbf{s}, \mathbf{D}, \mathbf{q}, \dot{\mathbf{q}})$ explicitly depends on system feature $\mathbf{s}$, intensity of excitation $2\mathbf{D}$, and state variables $\mathbf{q}$ and $\dot{\mathbf{q}}$. The assumption of exponential form guarantees the nonnegativity of stationary probability density. Our objective is to derive the explicitly analytical expression of the power from the approximate probability density at preset grids evaluated statistically from the simulated data.

2.3 Determination of nondimensional parameter clusters and expansion of power of exponential function

The power of exponential function $f(\mathbf{s}, \mathbf{D}, \mathbf{q}, \dot{\mathbf{q}})$ must be nondimensional, because an exponential function can be expressed as the power series of f. Thus, it is reasonable to first express the power $f(\mathbf{s}, \mathbf{D}, \mathbf{q}, \dot{\mathbf{q}})$ as a linear combination of a series of nondimensional parameter clusters which are constructed by system feature, intensity of excitation, and state variables. Here, we construct the nondimensional parameter clusters by *the rule of dimensional consistency* [27–29].

For general mechanical vibrating systems, there only exist three independent dimensions, i.e., the dimensions of mass, length, and time denoted by M, L, and T, respectively. The dimension of arbitrary quantity κ in mechanical systems can be expressed by these three basic dimensions, that is $[\kappa] = M^{\alpha}L^{\beta}T^{\gamma}$, in which α, β, γ are real constants. For the random vibrating systems, the dimensions of state variables $\mathbf{q}, \dot{\mathbf{q}}$ and system feature $\mathbf{s}$, such as mass, linear, or nonlinear stiffness coefficients, and linear or nonlinear damping coefficients are easily determined. The dimensions of intensities of excitations, however, are determined by the following relation $\left[D_{ij}\right] = [W_i][W_i]T$.

Preselect several quantities from system feature, intensity of excitation, and state variables to construct the nondimensional parameter clusters. The number of preselected quantities λ should be equal to or larger than 3 which is the number of independent dimensions, and the number of possible selections is $C^{\lambda}_{2n+l+m\times(m+1)/2}$. The powers of these preselected quantities can be obtained by solving homogeneous linear algebraic equations with three rows and λ columns. For each selection, the homogeneous linear algebraic equations may have a unique solution (i.e., zero solution) or infinite solutions. Zero solution corresponds to a nondimensional constant 1. The infinite solutions mean that there exist infinite ways to construct nondimensional quantities through the preselected quantities. For complicated systems, we tend to first select less quantities to construct the nondimensional parameter clusters. Only when the analytical results cannot satisfy the requirement of accuracy, we include more quantities in the construction of

nondimensional quantities. For simple systems, we directly select all the quantities to construct the nondimensional parameter clusters.

Then, the power of exponential function can be expanded as the linear combinations of the nondimensional parameter clusters, that is,

$$f(\mathbf{s},\mathbf{D},\mathbf{q},\dot{\mathbf{q}}) = \sum_i G_i \times g_i(\mathbf{s},\mathbf{D},\mathbf{q},\dot{\mathbf{q}}) \tag{3}$$

in which $g_i(\mathbf{s},\mathbf{D},\mathbf{q},\dot{\mathbf{q}})$ are the nondimensional parameter clusters which may include all or part of the system feature, intensity of excitation, and state variables. For the nondimensional parameter clusters with free index(es), we first set the free index(es) as small integers and then increase the values of free index(es) until the accuracy is satisfactory. Note that the nondimensional constant 1 is included in parameter clusters as an independent cluster. The coefficient of the nondimensional constant 1 corresponds to the normalization constant of the stationary probability density. The other undetermined nondimensional coefficients G_i can be regarded as the *characteristic values* of the system, which do not change with the values of system feature and intensity of excitation.

2.4 Criteria selection and optimization algorithm

Superficially, we should construct the total residual between the analytical probability density with exponential form and the approximate probability density statistically evaluated from the simulated data in full spatial domain and then determine the undetermined coefficients G_i by minimizing the residual. This procedure, however, will inevitably induce a complex solving problem of nonlinear algebraic equations. Alternatively, we can bypass this difficulty by comparing the power of exponential form of stationary probability density $f(\mathbf{s},\mathbf{D},\mathbf{q},\dot{\mathbf{q}})$ and the approximate logarithm probability density $\ln[\hat{p}_s(\mathbf{s},\mathbf{D},\mathbf{q},\dot{\mathbf{q}})]$. The residual in a prescribed spatial domain Ω is defined as,

$$\begin{aligned}\varepsilon &= \iint_\Omega \{f(\mathbf{s},\mathbf{D},\mathbf{q},\dot{\mathbf{q}}) - \ln[\hat{p}_s(\mathbf{s},\mathbf{D},\mathbf{q},\dot{\mathbf{q}})]\}^2 \mathrm{d}\mathbf{q}\mathrm{d}\dot{\mathbf{q}} \\ &= \iint_\Omega \left\{\sum_i G_i \times g_i(\mathbf{s},\mathbf{D},\mathbf{q},\dot{\mathbf{q}}) - \ln[\hat{p}_s(\mathbf{s},\mathbf{D},\mathbf{q},\dot{\mathbf{q}})]\right\}^2 \mathrm{d}\mathbf{q}\mathrm{d}\dot{\mathbf{q}}\end{aligned} \tag{4}$$

Minimizing the residual yields the linear algebraic relations with respect to undetermined coefficients G_i, i.e.,

$$\begin{aligned}&\iint_\Omega \left\{\sum_j G_j \times g_j(\mathbf{s},\mathbf{D},\mathbf{q},\dot{\mathbf{q}}) - \ln[\hat{p}_s(\mathbf{s},\mathbf{D},\mathbf{q},\dot{\mathbf{q}})]\right\} \\ &\quad \times g_i(\mathbf{s},\mathbf{D},\mathbf{q},\dot{\mathbf{q}})\mathrm{d}\mathbf{q}\mathrm{d}\dot{\mathbf{q}}, \\ &\quad i = 1,2\ldots\end{aligned} \tag{5}$$

The number of linear relations just matches with the number of undetermined coefficients G_i. Solving the simultaneous linear algebraic equations gives the optimal values of the undetermined coefficients G_i^*. Note that the integral expression must be calculated numerically because the approximate probability density $\hat{p}_s(\mathbf{s},\mathbf{D},\mathbf{q},\dot{\mathbf{q}})$ is only given in preset grids. It is worth pointing out that for an arbitrarily prescribed spatial domain, we can establish a set of linear algebraic equations with the same number of undetermined coefficients G_i. If the full spatial domain is deliberately partitioned into several subdomains, we will obtain plenty of linear algebraic equations with the number significantly larger than that of G_i. If the exact data are adopted, the number of the *independent* equations just equals to the number of G_i, and so the deliberate partition of the spatial domain is insignificant. However, for the approximate probability density at preset grids evaluated statistically, the deliberate partition is of great significance. The optimal values of undetermined coefficients can be obtained by the pseudo-inverse algorithm, which can dramatically reduce the influence of the error induced by the statistical calculation from a small amount of simulated data. Furthermore, the number of the overdetermined equations can be further enlarged by using the statistically evaluated approximate probability densities of the same system with different values of system feature and intensity of excitations.

In the approximate probability density statistically evaluated from the simulated data, it is possible that there exist some grids with the probability density value just being zero. Due to the singularity of the logarithm of real numbers close to 0, the small domains including these grids should be excluded from the integral domain in Eq. (5). In addition, compared to the criterion with respect to the probability density itself, the criterion with respect to the logarithm probability density means assigning large weight at the domain near to the edge of probability

density. Thus, the probability density obtained will be more accurate at the edge, which is of great significance for the analysis and design for reliability. So far, the (approximately) analytical expression of the stationary probability density of nonlinear random vibrating systems can be derived by solving a set of (overdetermined) linear algebraic equations, no matter how complex the system concerned. The flow diagrams of the data-driven method are depicted in Fig. 2.

3 Numerical example: Duffing oscillator

In this section, we concentrate on the famous nonlinear system, i.e., Duffing oscillator, and derive the stationary probability density from the simulated data by the data-driven method. The exact stationary probability density of Duffing oscillator is known, and so it can be used as a benchmark problem to assess the efficacy of the data-driven method.

Consider a Duffing oscillator subjected to external Gaussian white noise excitation. The equation of motion is as,

$$m\ddot{q} + c\dot{q} + k_1 q + k_3 q^3 = W(t) \tag{6}$$

in which m and c are the mass of block and linear damping coefficient, respectively. k_1 and k_3 are linear and nonlinear stiffness coefficients, respectively. The intensity of excitation is denoted by $2D$.

The dimensions of the system feature (i.e., mass, damping coefficient, stiffness coefficients), intensity of excitation, state variables (i.e., displacement and velocity) are listed in Table 1. For this simple system, we directly select all these quantities to construct nondimensional parameter clusters. From the rule of dimensional consistency, we have $M^0L^0T^0 = [m]^i[c]^j[k_1]^k[k_3]^l[D]^s[q]^\tau[\dot{q}]^r$. The powers satisfy the following homogeneous linear algebraic equations, i.e.,

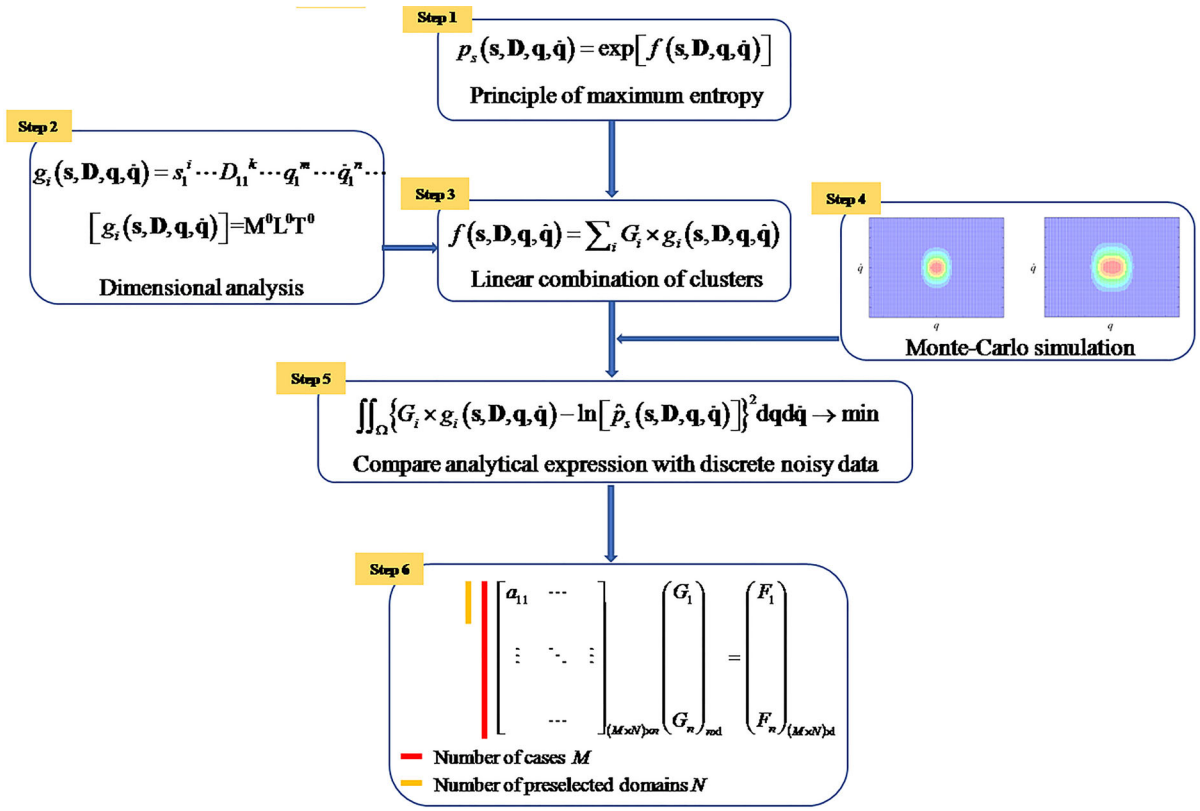

Fig. 2 Flow diagrams of the data-driven method

Table 1 Dimensions of system feature, intensity of excitation, and state variables of Duffing oscillator

	$s_1(m)$	$s_2(c)$	$s_3(k_1)$	$s_4(k_3)$	$s_5(D)$	q	$\dot{q}$	$f(\mathbf{s}, D, q, \dot{q})$
M	1	1	1	1	2	0	0	0
L	0	0	0	− 2	2	1	1	0
T	0	− 1	− 2	− 2	− 3	0	− 1	0

$$i+j+k+l+2s=0,\quad -2l+2s+\tau+r=0,\quad -j-2k-2l-3s-r=0 \tag{7}$$

The powers s, τ and r can be represented by the other four powers i, j, k and l by solving the above linear equations. Then, the nondimensional parameter clusters can be expressed as,

$$m^i c^j k_1^k k_3^l D^{-\frac{i+j+k+l}{2}} q^{\frac{-i+j+3k+7l}{2}} \dot{q}^{\frac{3i+j-k-l}{2}} \tag{8}$$

According to the principle of simplicity, we first select the free variables i, j, k and l, as 1, 0, − 1. By deleting the singular terms and complex terms, the nondimensional parameter clusters are reduced as,

$$\begin{aligned} &1,\quad ck_1D^{-1}q^2,\quad k_1^{-1}k_3q^2,\quad ck_3D^{-1}q^4,\\ &mc^{-1}k_1k_3D^{-1}q^4,\quad mk_1D^{-1}q\dot{q},\quad mc^{-1}k_1^{-1}k_3q\dot{q},\\ &mk_3D^{-1}q^3\dot{q}, mck_1k_3D^{-2}q^5\dot{q},\quad mcD^{-1}\dot{q}^2,\\ &mck_1^{-1}k_3D^{-1}q^2\dot{q}^2 \end{aligned} \tag{9}$$

These parameter clusters will be cited as $g_j(\mathbf{s}, D, q, \dot{q})$ in what follows. The power of the assumed exponential function of stationary probability density is then expanded as the linear combinations of the nondimensional parameter clusters. That is,

$$\begin{aligned} &f(\mathbf{s}, D, q, \dot{q})\\ &=\sum_{j=0}^{10} G_j \times g_j(\mathbf{s}, D, q, \dot{q})\\ &= G_0\times 1 + G_1\times ck_1D^{-1}q^2 + G_2\times k_1^{-1}k_3q^2\\ &\quad + G_3\times ck_3D^{-1}q^4 + G_4\times mc^{-1}k_1k_3D^{-1}q^4\\ &\quad + G_5\times mk_1D^{-1}q\dot{q} + G_6\times mc^{-1}k_1^{-1}k_3q\dot{q}\\ &\quad + G_7\times mk_3D^{-1}q^3\dot{q} + G_8\times mck_1k_3D^{-2}q^5\dot{q}\\ &\quad + G_9\times mcD^{-1}\dot{q}^2 + G_{10}\times mck_1^{-1}k_3D^{-1}q^2\dot{q}^2 \end{aligned} \tag{10}$$

in which $G_j(i=0,1,\ldots 10)$ are the undetermined coefficients associated with the parameter clusters $g_j(\mathbf{s}, D, q, \dot{q})$.

The undetermined coefficients $G_j(i=0,1,\ldots 10)$ satisfy the following simultaneous linear algebraic equations,

$$\begin{aligned} &\sum_{j=0}^{10}\left[\iint_{\Omega} g_j(\mathbf{s}, D, q, \dot{q})\times g_i(\mathbf{s}, D, q, \dot{q})\mathrm{d}q\mathrm{d}\dot{q}\right]\\ &G_j = \iint_{\Omega} \ln[\hat{p}_s(\mathbf{s}, D, q, \dot{q})]\times g_i(\mathbf{s}, D, q, \dot{q})\mathrm{d}q\mathrm{d}\dot{q}\\ &\quad (i=0,1,\ldots 10) \end{aligned} \tag{11}$$

Note that $g_1/g_2 = ck_1^2D^{-1}k_3^{-1}, g_3/g_4 = c^2m^{-1}k_1^{-1}$, $g_5/g_6 = k_1^2D^{-1}ck_3^{-1}$ are independent on state variables $q, \dot{q}$. Thus, for a set of given values of system feature and intensity of excitation, the coefficients of G_1, G_3, G_5 are proportional to G_2, G_4, G_6, respectively, regardless of the selection of the prescribed spatial domain. Here, we develop the following procedure to derive the undetermined coefficients by using the statistically evaluated approximate probability densities from several cases, i.e., the same system with different values of system feature and intensity of excitation.

We first combine the nondimensional parameter clusters with the same power of state variables. The expression of the power of stationary probability density in Eq. (10) is then rearranged as,

$$\begin{aligned} &f(\mathbf{s}, D, q, \dot{q})\\ &= G_0\times 1 + P_1\times q^2 + P_2\times q^4 + P_3\times q\dot{q}\\ &\quad + G_7\times mk_3D^{-1}q^3\dot{q} + G_8\times mck_1k_3D^{-2}q^5\dot{q}\\ &\quad + G_9\times mcD^{-1}\dot{q}^2 + G_{10}\times mck_1^{-1}k_3D^{-1}q^2\dot{q}^2 \end{aligned} \tag{12}$$

with $P_1 = G_1ck_1D^{-1} + G_2k_1^{-1}k_3, P_2 = G_3ck_3D^{-1} + G_4mc^{-1}k_1k_3D^{-1}, P_3 = G_5mk_1\quad D^{-1} + G_6mc^{-1}k_1^{-1}k_3$. For an arbitrarily selected set of values of system feature and intensity of excitation, we can derive a set of values of $G_0, P_1, P_2, P_3, G_7, G_8, G_9, G_{10}$. The coefficients G_7, G_8, G_9, G_{10} are independent to system feature and intensity of excitation. The coefficient G_0

Table 2 Values of system parameters of Duffing oscillator for two cases

	m	c	k_1	k_3	D
Case I	1.0	0.5	1.5	2.5	0.5
Case II	1.0	1.0	0.5	1.5	1.5

which corresponding to the normalization condition is usually different for different values of system feature and intensity of excitation. The coefficients $G_1, G_2, G_3, G_4, G_5, G_6$ which are independent to system feature and intensity of excitation can be solved from the definition of P_i and the values P_i for several cases by using the Gaussian elimination method (for two cases) or pseudo-inverse algorithm (for three or more cases).

Here, the statistically evaluated approximate probability densities from two cases are adopted to determine the characteristic quantities $G_j (i = 0, 1, \ldots 10)$. The values of system feature and intensity of excitation are listed in Table 2. The approximate values of probability densities with the grid spacing $1/10 \times 1/10$ are evaluated statistically from two hundred million simulated data, as shown in Fig. 3a, b. Denote the maximum value of $\hat{p}_s(\mathbf{s}, D, q, \dot{q})$ as $\hat{p}_{\max}(\mathbf{s}, D)$, and we select the spatial domain with the approximate values of probability densities larger than $\alpha \hat{p}_{\max}(\mathbf{s}, D)$ to derive the undetermined coefficients. Here, $0 < \alpha \leq 1$, and the smaller the value of α the larger the domain utilized.

Set α being 0.01, and the data adopted are shown in the upper two contour figures of Fig. 4. From the data of Case I, we obtain $G_0 = -1.36$, $P_1 = -0.757$, $P_2 = -0.615$, $P_3 = -8.57 \times 10^{-5}$, $G_7 = -1.03 \times 10^{-4}$, $G_8 = 8.11 \times 10^{-5}$, $G_9 = -0.501$, $G_{10} = 1.81 \times 10^{-4}$, while from the data of Case II, $G_0 = -1.96$, $P_1 = -0.167$, $P_2 = -0.249$, $P_3 = 2.81 \times 10^{-5}$, $G_7 = -5.36 \times 10^{-5}$, $G_8 = 1.29 \times 10^{-4}$, $G_9 = -0.502$, $G_{10} = -1.81 \times 10^{-4}$. From the values of P_i in these two cases, we obtain $G_1 = -0.505$, $G_2 = 5.84 \times 10^{-4}$, $G_3 = -0.249$, $G_4 = 5.66 \times 10^{-4}$, $G_5 = -4.44 \times 10^{-5}$, $G_6 = 1.43 \times 10^{-5}$.

Then, the analytical expression of the stationary probability density of Duffing oscillator derived from the data-driven method is as,

$$\begin{aligned} & p_s(s, D, q, \dot{q}) \\ & = \exp[f(s, D, q, \dot{q})] = \exp[G_0] \cdot \exp[-0.505 c k_1 D^{-1} q^2 \\ & \quad + 5.84 \times 10^{-4} k_1^{-1} k_3 q^2 - 0.249 c k_3 D^{-1} q^4 \\ & \quad + 5.66 \times 10^{-4} m c^{-1} k_1 k_3 D^{-1} q^4 - 4.44 \times 10^{-5} m k_1 D^{-1} q \dot{q} \\ & \quad + 1.43 \times 10^{-5} m c^{-1} k_1^{-1} k_3 q \dot{q} - 1.03 \times 10^{-4} m k_3 D^{-1} q^3 \dot{q} \\ & \quad + 8.11 \times 10^{-5} m c k_1 k_3 D^{-2} q^5 \dot{q} - 0.501 \times m c D^{-1} \dot{q}^2 \\ & \quad + 1.81 \times 10^{-4} m c k_1^{-1} k_3 D^{-1} q^2 \dot{q}^2] \end{aligned} \tag{13}$$

By neglecting the quantities with small order of magnitude, it is obvious that the derived stationary probability density agrees very well with the well-known analytical expression,

$$p(q, \dot{q}) = C \exp\left[-\frac{c}{D}\left(\frac{1}{2} m \dot{q}^2 + \frac{1}{2} k_1 q^2 + \frac{1}{4} k_3 q^4\right)\right] \tag{14}$$

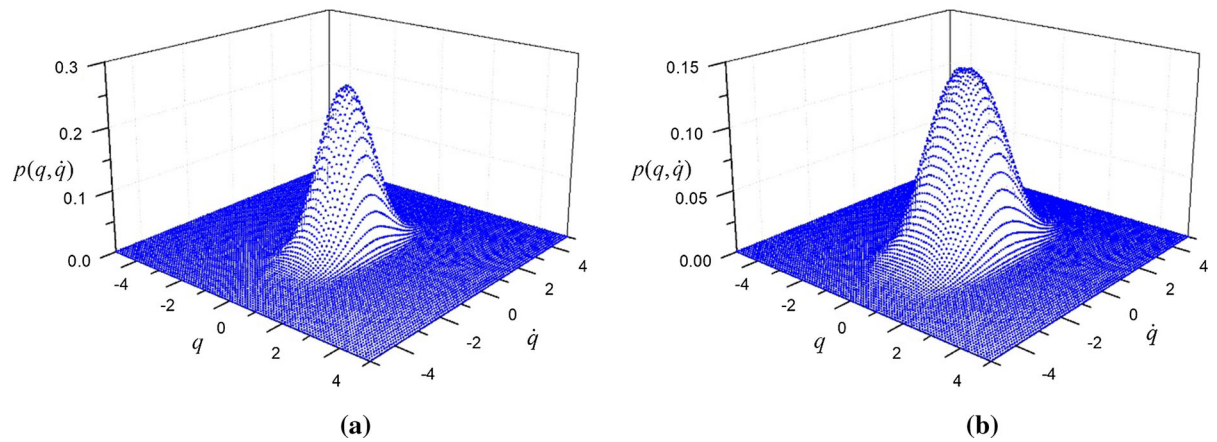

(a) **(b)**

Fig. 3 Statistically evaluated approximate stationary probability density of Duffing oscillator (with grid spacing $1/10 \times 1/10$). **a** Case I; **b** Case II

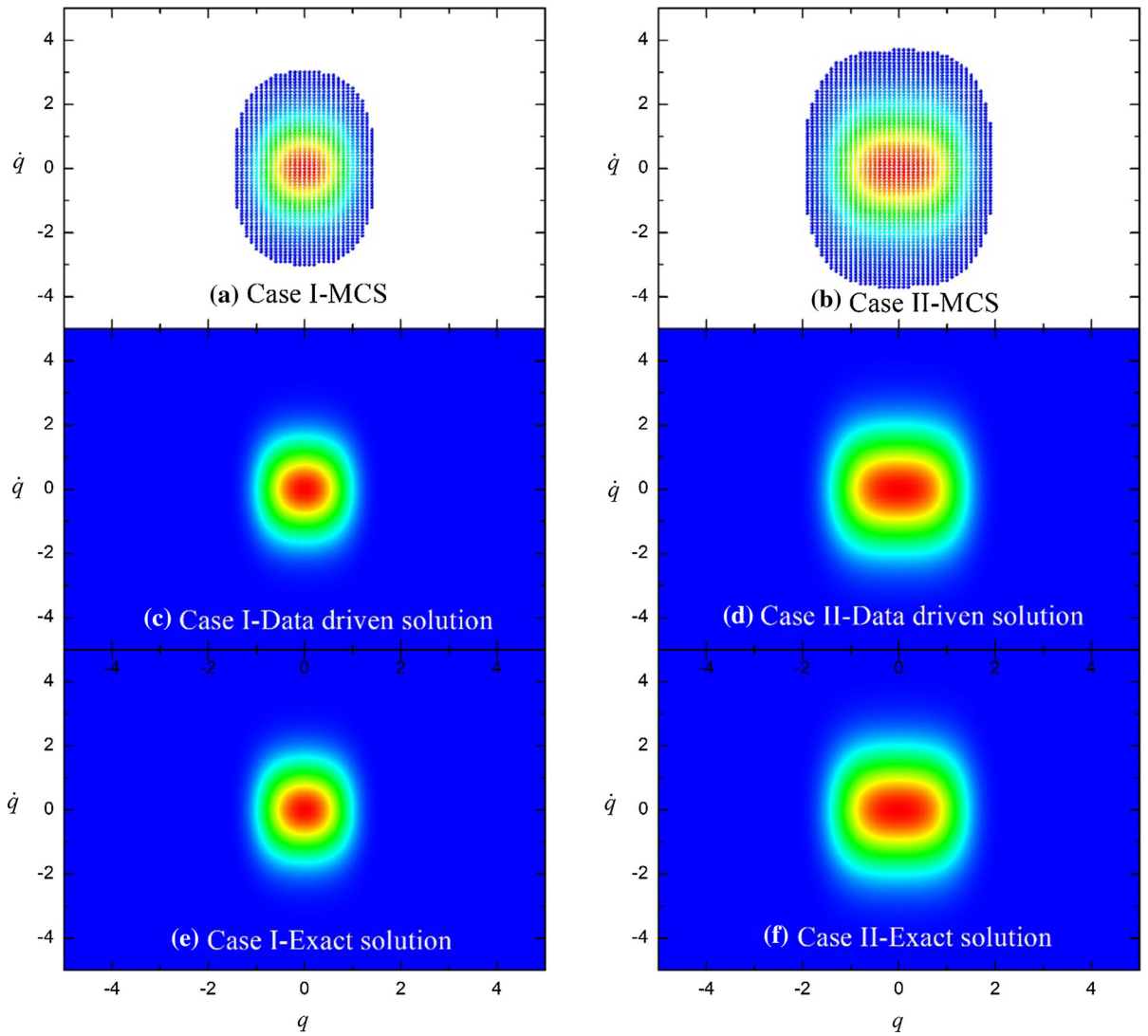

Fig. 4 Contour maps of stationary probability density of Duffing oscillator. **a** Approximate probability density of Case I ($\alpha = 0.01$); **b** approximate probability density of Case II ($\alpha = 0.01$); **c** derived solution of Case I from data-driven method; **d** derived solution of Case II from data-driven method; **e** exact solution of Case I; **f** exact solution of Case II

The contour maps of the derived expression from the data-driven method in Eq. (13) and the analytical expression in Eq. (14) are depicted in the middle two figures and the lower two figures of Fig. 4, respectively. The data-driven method identifies the analytical expression of the stationary probability density with high accuracy from the simulated data. Figure 5 depicts the data adopted as $\alpha = 0.25$ (as shown in the upper two figures) and the contour maps of the derived results from data-driven method (as shown in the lower two figures). Figure 6 gives the associated results as $\alpha = 0.5$.

To evaluate the identified accuracy of the data-driven method, an error of the identified result to the analytical result is defined as,

$$R = \frac{\sum_{i=1}^{10} (G_i - a_i)^2}{\sum_{i=1}^{10} a_i^2} \tag{15}$$

in which $a_1 = -\frac{1}{2}$, $a_3 = -\frac{1}{4}$, $a_9 = -\frac{1}{2}$ which are the effective coefficients in analytical expression in Eq. (14), while $a_i = 0 (i \neq 1, 3, 9)$. The data-driven

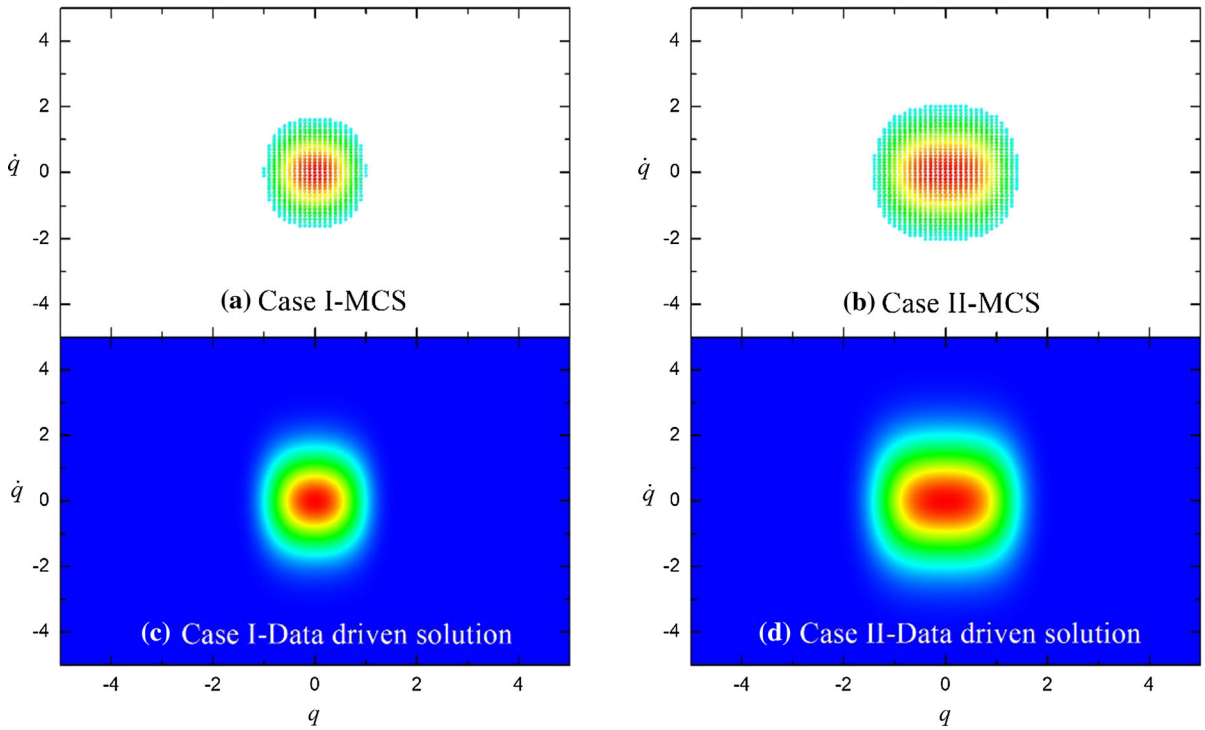

Fig. 5 Contour maps of stationary probability density of Duffing oscillator. **a** Approximate probability density of Case I ($\alpha = 0.25$); **b** approximate probability density of Case II ($\alpha = 0.25$); **c** derived solution of Case I from data-driven method; **d** derived solution of Case II from data-driven method

method gives analytical expression of stationary probability density with high accuracy up to $\alpha = 0.75$, as shown in Fig. 7. Figure 8 depicts the dependence of the error of data-driven method on the number of simulated data from which the approximate probability densities at preset grids are evaluated statistically. The error monotonically decreases with the increase in the number of simulated data. Furthermore, by using the exact approximate probability densities at preset grids, the analytical expression identified by the data-driven method is almost completely consistent with the exact stationary probability density in Eq. (14).

4 Numerical example: van der Pol system

In this section, we concentrate on the van der Pol system excited by Gaussian white noise, which is an important nonlinear system in the field of nonlinear dynamics. It comes from a circuit system including semiconductor, capacitance, inductance, and battery and now has been realized in mechanical system [30]. So far, the analytical expression of the stationary probability density of van der Pol system has not been derived.

The equation of motion of van der Pol system is expressed as,

$$m\ddot{q} + \left(c_1 + c_2 q^2\right)\dot{q} + kq = W(t) \tag{16}$$

in which m is the mass of block, k is linear stiffness coefficient. $c_1 < 0$ and $c_2 > 0$ are linear and nonlinear damping coefficients, respectively. $W(t)$ is Gaussian white noise with intensity $2D$.

The dimensions of system feature, intensity of excitation, and state variables are listed in Table 3. We select all quantities to construct the nondimensional parameter clusters. From the rule of dimensional consistency, we have $M^0L^0T^0 = [m]^i[c_1]^j[c_2]^\eta [k]^l[D]^s[q]^\tau[\dot{q}]^r$. The powers satisfy the following homogeneous linear algebraic equations, i.e.,

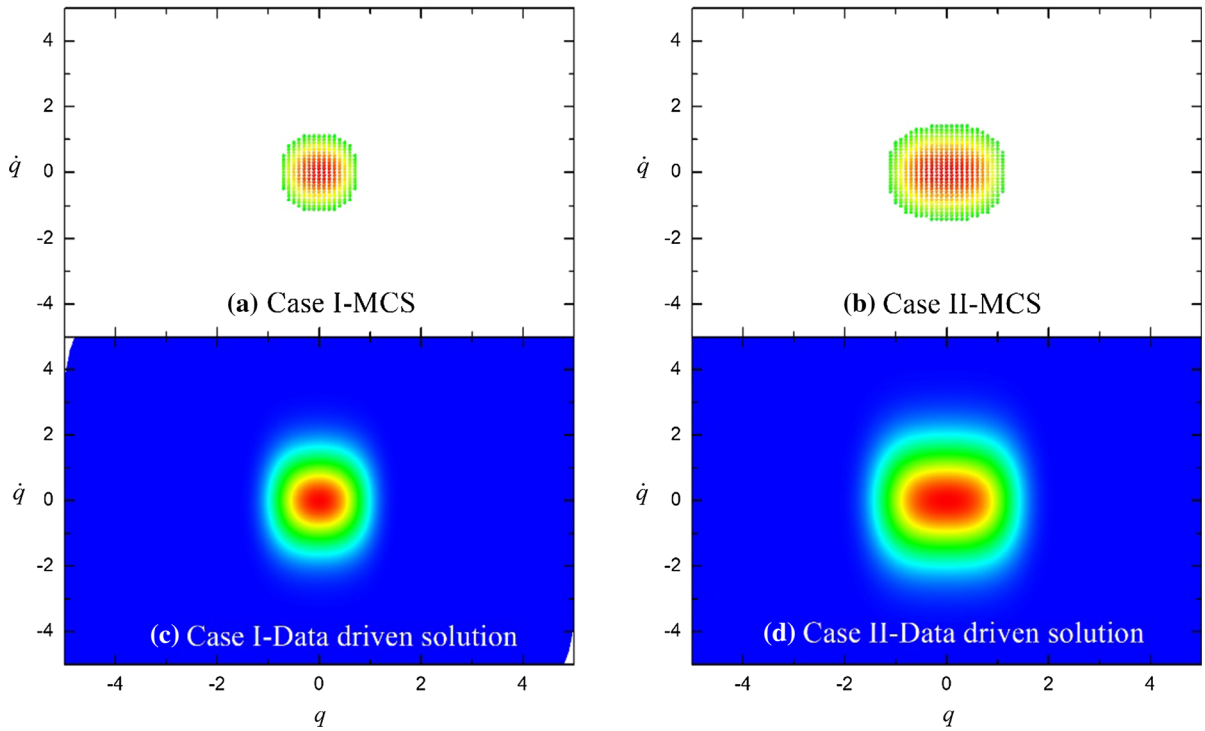

Fig. 6 Contour maps of stationary probability density of Duffing oscillator. **a** Approximate probability density of Case I ($\alpha = 0.5$); **b** approximate probability density of Case II ($\alpha = 0.5$); **c** derived solution of Case I from data-driven method; **d** derived solution of Case II from data-driven method

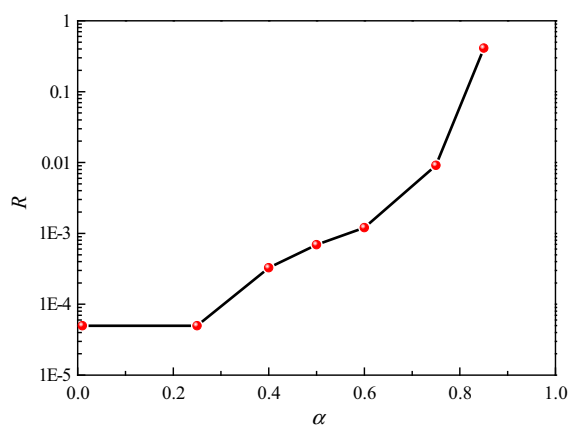

Fig. 7 Dependence of the error R on the value of parameter α

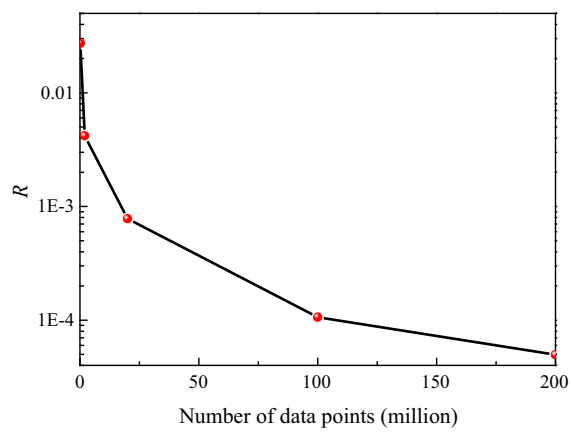

Fig. 8 Dependence of the error R on the number of data points

$$i + j + \eta + l + 2s = 0, \quad -2\eta + 2s + \tau + r = 0, \quad -j - \eta - 2l - 3s - r = 0 \tag{17}$$

The indexes s, τ, and r can be represented by the other four indexes i, j, η, and l. Then the nondimensional parameter clusters are expressed as,

$$m^i c_1^j c_2^\eta k^l D^{-\frac{i+j+\eta+l}{2}} q^{\frac{-i+j+5\eta+3l}{2}} \dot{q}^{\frac{3i+j+\eta-l}{2}} \tag{18}$$

Set the free indexes i, j, η, and l as -2, -1, 0, 1, 2, and retain the nondimensional parameter clusters with the power of state variables not higher than 4. The number of the nondimensional parameter clusters $g_j(\mathbf{s}, D, q, \dot{q})$ is 45. The power of the exponential

expression of stationary probability density is then expressed as the linear combinations, $f(\mathbf{s}, D, q, \dot{q}) = \sum_{j=0}^{44} G_j \times g_j(\mathbf{s}, D, q, \dot{q})$.

Careful observation shows that we can use the data from six cases to determine the undetermined coefficients $G_j (j = 0, 1\ldots, 44)$. The values of system feature and intensity of excitation for these six cases are shown in Table 4. The approximate stationary probability densities for each case are evaluated statistically from two hundred million simulated data, just as shown in Fig. 9. By setting the parameter α being 0.01, the analytical expression of the stationary probability density identified by the data-driven method is as,

$$
\begin{aligned}
p(x,\dot{x}) = \exp[G_0] \times \exp[&4.32 \times 10^{-2} c_1^{-1} c_2 q^2 \\
&- 0.327 c_1 k_1 D^{-1} q^2 - 0.118 m^{-1} c_1^{-1} c_2^2 k_1^{-2} D q^2 \\
&- 9.66 m^{-1} c_1 c_2 k_1^{-1} q^2 - 6.25 \times 10^{-4} c_1^{-2} c_2^2 q^4 \\
&- 6.50 \times 10^{-2} c_2 k_1 D^{-1} q^4 + 4.55 \times 10^{-4} c_1^2 k_1^2 D^{-2} q^4 \\
&+ 1.77 \times 10^{-3} m^{-2} c_1^2 c_2^2 k_1^2 q^4 + 9.12 \\
&\times 10^{-2} m^{-1} c_1^2 c_2 D^{-1} q^4 - 5.73 \times 10^{-2} m^{-1} c_2^2 k_1^{-1} q^4 \\
&+ 1.28 \times 10^{-5} m c_1^{-2} c_2 k_1^2 D^{-1} q^4 \\
&- 0.721 c_1^2 D^{-1} q\dot{q} + 4.78 \times 10^{-3} c_1^{-2} c_2^2 k_1^{-2} D q\dot{q} \\
&- 1.14 k_1^{-1} c_2 q\dot{q} - 4.28 \times 10^{-2} m^{-1} c_1^2 c_2 k_1^{-2} q\dot{q} \\
&- 5.57 \times 10^{-5} m c_1^{-2} c_2 q\dot{q} \\
&- 1.95 \times 10^{-4} m k_1 D^{-1} q\dot{q} + 1.74 \\
&\times 10^{-3} m c_1^2 c_2^{-1} k_1^2 D^{-2} q\dot{q} - 2.84 \\
&\times 10^{-5} m^2 c_1^{-2} k_1^2 D^{-1} q\dot{q} - 0.144 c_1 c_2 D^{-1} q^3 \dot{q} \\
&- 1.39 \times 10^{-2} c_1^{-1} c_2^2 k_1^{-1} q^3 \dot{q} + 0.683 m^{-1} c_1 c_2^2 q^3 \dot{q} \\
&- 6.57 \times 10^{-4} m c_1^{-1} c_2 k_1 D^{-1} q^3 \dot{q} + 2.70 \\
&\times 10^{-4} m c_1 k_1^2 D^{-2} q^3 \dot{q} - 9.91 c_1 c_2 k_1^{-2} \dot{q}^2 \\
&- 0.274 m c_1 D^{-1} \dot{q}^2 + 5.51 \times 10^{-2} m c_1^{-1} c_2 k_1^{-1} \dot{q}^2 \\
&- 1.09 \times 10^{-3} m^2 c_1^{-1} k_1 D^{-1} \dot{q}^2 \\
&- 1.71 \times 10^{-4} m^2 c_1 c_2^{-1} k_1^2 D^{-2} \dot{q}^2 - 0.147 c_2^{-2} k_1^2 q^2 \dot{q}^2 \\
&- 9.69 \times 10^{-2} c_1^2 c_2 k_1^{-1} D^{-1} q^2 \dot{q}^2 \\
&- 0.125 m c_2 D^{-1} q^2 \dot{q}^2 - 7.40 \times 10^{-4} m c_1^{-2} c_2^2 k_1^{-1} q^2 \dot{q}^2 \\
&+ 2.00 \times 10^{-3} m c_1^2 k_1 D^{-2} q^2 \dot{q}^2 - 2.95 \\
&\times 10^{-5} m^2 c_1^{-2} c_2 k_1 D^{-1} q^2 \dot{q}^2 + 3.12 \\
&\times 10^{-6} m^2 k_1^2 D^{-2} q^2 \dot{q}^2 - 1.38 \times 10^{-2} m c_1^{-1} c_2^2 k_1^{-2} q\dot{q}^3 \\
&- 0.284 m c_1 c_2 k_1^{-1} D^{-1} q\dot{q}^3 - 2.62 m^2 c_1^{-1} c_2 D^{-1} q\dot{q}^3 \\
&+ 1.03 \times 10^{-3} m^2 c_1 k_1 D^{-2} q\dot{q}^3 + 0.221 m c_1^2 c_2 k_1^{-2} D^{-1} \dot{q}^4 \\
&- 1.53 \times 10^{-4} m^2 c_1^2 D^{-2} \dot{q}^4 + 3.40 \times 10^{-4} m^2 c_1^{-2} c_2^2 k_1^{-2} \dot{q}^4 \\
&- 6.17 \times 10^{-2} m^2 c_2 k_1^{-1} D^{-1} \dot{q}^4]
\end{aligned}
\tag{19}
$$

The contour maps of the data adopted and the results derived from the data-driven method are depicted for comparison, as shown in Fig. 10. The upper six figures represent the data adopted, while the lower six figures represent the results derived from the data-driven method. The stationary probability densities identified by the data-driven method agree very well with the approximate probability densities from those the analytical expression in Eq. (19) is derived.

Define the error of the derived solution from the data-driven method to a reference solution, that is,

$$
R = \frac{\iint \left[p(q,\dot{q}) - p_{ref}(q,\dot{q})\right]^2 \mathrm{d}q\mathrm{d}\dot{q}}{\iint \left[p_{ref}(q,\dot{q})\right]^2 \mathrm{d}q\mathrm{d}\dot{q}} \tag{20}
$$

in which $p(q,\dot{q}) = \exp[f(\mathbf{s}, D, q, \dot{q})]$ is the derived probability density by the data-driven method. Here, we adopt the numerical solution of the associated reduced FPK equation as the reference result $p_{\mathrm{ref}}(q,\dot{q})$. The reduced FPK equation associated with the van der Pol system is as,

$$
-\dot{q}\frac{\partial p}{\partial q} + \frac{1}{m}\frac{\partial}{\partial \dot{q}}\left\{\left[(c_1 + c_2 q^2)\dot{q} + kq\right]p\right\} + \frac{D}{m^2}\frac{\partial^2 p}{\partial \dot{q}^2} = 0 \tag{21}
$$

The dependence of the error R on the value of parameter α is depicted in Fig. 11. The data-driven method gives the analytical expression with high accuracy even for large value of α. Figure 12 depicts the dependence of the error R on the number of simulated data from which the approximate probability density is evaluated statistically. The error monotonically decreases with the increase in the number of simulated data which corresponds to the increase in the accuracy of the approximate probability density. The analytical expression in Eq. (19) is obtained from the simulated data of six specific cases. Although it is not the exact analytical solution, we participate it provides good approximation of van der Pol system with values of system feature and intensity of excitation which is not deviating those of six specific cases prominently. Select the values of system attribute and intensity of excitation of Case III as the baseline. Figure 13a, b depicts the dependences of the error R on the variation of mass and linear damping coefficient, respectively. The analytical expression from data-driven method gives the approximation of stationary probability density with acceptable accuracy for a

Table 3 Dimensions of system feature, intensity of excitation, and state variables of van der Pol system

	$s_1(m)$	$s_2(c_1)$	$s_3(c_2)$	$s_3(k)$	$s_5(D)$	q	$\dot{q}$	$f(\mathbf{s}, D, q, \dot{q})$
M	1	1	1	1	2	0	0	0
L	0	0	− 2	0	2	1	1	0
T	0	− 1	− 1	− 2	− 3	0	− 1	0

Table 4 Values of system parameters of van der Pol system for six cases

	m	c_1	c_2	k	D
Case I	1.0	− 0.1	0.3	2.0	0.4
Case II	1.0	− 0.15	0.25	3.0	0.1
Case III	1.0	− 0.2	0.2	1.5	0.2
Case IV	1.0	− 0.25	0.15	2.5	0.5
Case V	1.0	− 0.3	0.1	1.0	0.05
Case VI	1.0	− 0.05	0.4	0.5	0.25

considerable range of variation of system feature and intensity of excitation.

5 Conclusion and discussion

A data-driven method is established to derive the (approximately) analytical expression of the stationary probability density of nonlinear random vibrating system, which comes down to the solution of (overdetermined) simultaneous linear algebraic equations. The exact analytical expression of the stationary probability density of random-excited Duffing oscillator can be rediscovered. For van der Pol system, the approximately analytical expression of the stationary probability density is obtained from the simulated data of six cases with different values of system feature and intensity of excitation, which is effective for a considerable range of parameter variation.

By using the rule of dimensional consistency, the derived analytical expression explicitly includes system feature and intensity of excitation. The data-driven method is the unique method which can explicitly include the information of system itself and excitation. Compared to the MCS method which is time-consuming and can only give the discrete values at preset grids, the data-driven method yields the analytical expression of the stationary probability density. By comparing the power of exponential function with the approximate logarithm probability density, the data-driven method comes down to the solution of simultaneous linear algebraic equations, which is easier than other existing methods, such as the maximum entropy method and the closure methods which correspond to the solution of simultaneous nonlinear algebraic equations.

Furthermore, the data-driven method starts from the simulated data of the original NSDEs; thus, there is not any limitation on the styles of random excitations and the styles of nonlinearity. This method, in theory, can be used to derive the stationary probability density for nonlinear systems with general random excitations. For instance, for the nonlinear systems with combined excitation of Gaussian white noise and harmonic force, the amplitude and circular frequency of harmonic force participate the construction of nondimensional parameter clusters. Furthermore, it is worth pointing out that the procedure of determining nondimensional parameter clusters can be generalized, i.e., deliberately add arbitrary functions of dimensionless parameter clusters as new parameter clusters if any prior knowledge is provided. This generalization is of great significance for complex nonlinear systems (e.g., hysteretic systems and frictional systems), in which the appropriate supplement of some specific parameter clusters will dramatically decrease the term number needed by the power expansion and prominently improve the efficiency of the data-driven method.

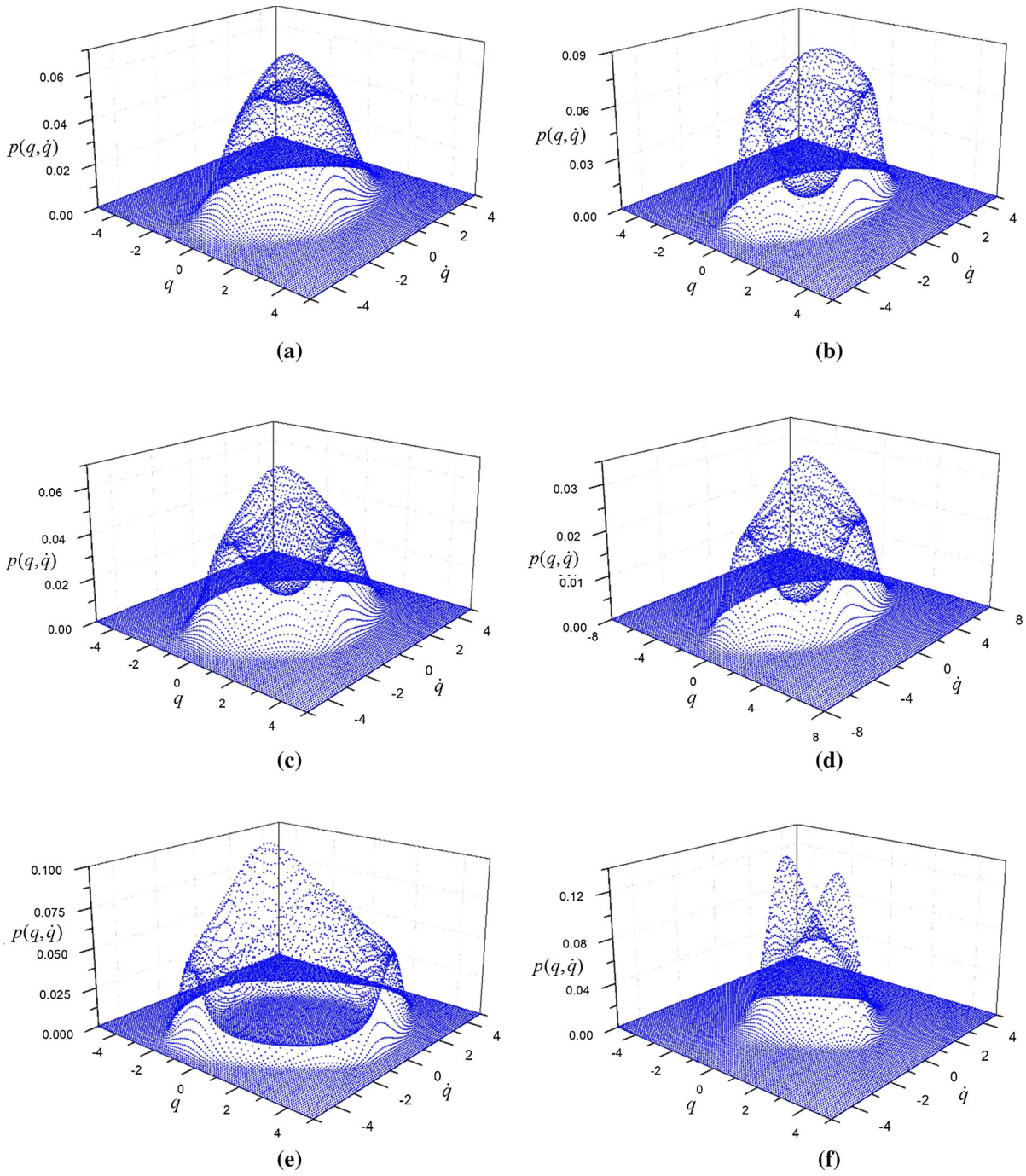

Fig. 9 Statistically evaluated approximate stationary probability density of van der Pol system. **a** Case I; **b** Case II; **c** Case III; **d** Case IV; **e** Case V; **f** Case VI

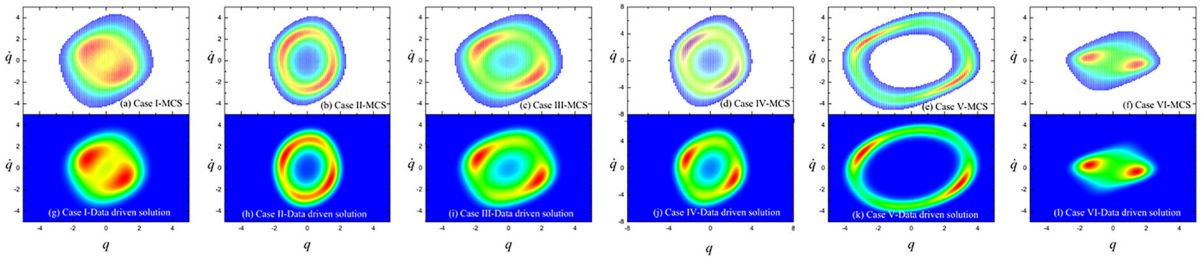

Fig. 10 Contour maps of stationary probability density of van der Pol system. The upper six figures depict the approximate probability density for Cases I–VI ($\alpha = 0.01$); the lower six figures depict the derived solution for Cases I–VI

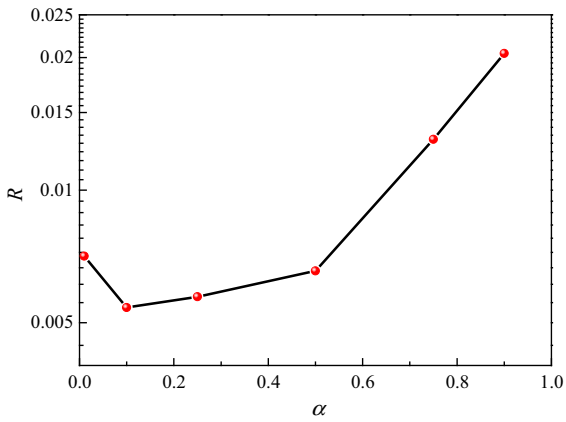

Fig. 11 Dependence of the error R on the value of parameter α

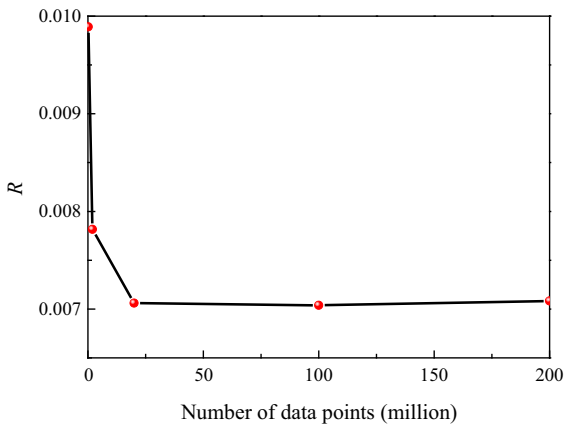

Fig. 12 Dependence of the error R on the number of data points

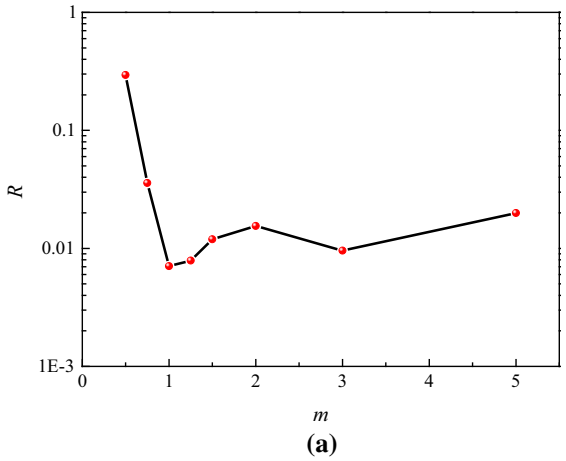

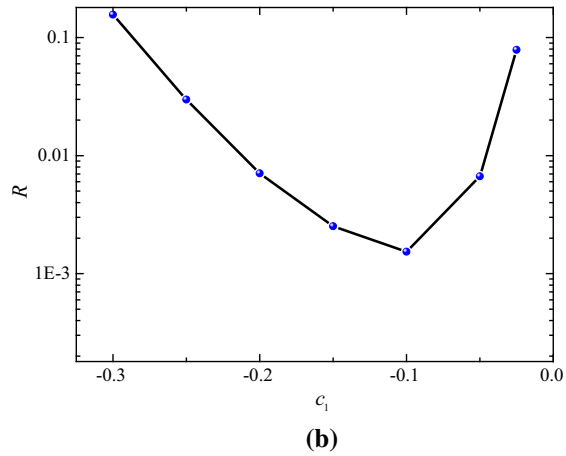

Fig. 13 Dependences of the error R on mass and linear damping coefficient. **a** Mass; **b** linear damping coefficient

Funding This study was supported by the National Natural Science Foundation of China under Grant Nos. 11872328, 11532011, 11972317, and 11621062 and the Fundamental Research Funds for the Central Universities under Grant No. 2018FZA4025.

Compliance with ethical standards

Conflict of interest The authors declare that they have no conflict of interest.

References

1. Lutes, L.D., Sarkani, S.: Random Vibrations: Analysis of Structural and Mechanical Systems. Elsevier, Butterworth-Heinemann (2004)
2. Sobczyk, K.: Stochastic dynamics of engineering systems: origins, challenges and results. In: Gutkowski, W., Kowalewski, T.A. (eds.) Mechanics of the 21st Century, pp. 19–60. Springer, Netherlands (2005)
3. Lin, Y.K., Cai, G.Q.: Probabilistic Structural Dynamics: Advanced Theory and Application. McGraw-Hill, New York (1995)
4. Zhu, W.Q., Cai, G.Q.: Elements of Stochastic Dynamics. World Scientific, Hackensack (2017)
5. Ibrahim, R.A.: Nonlinear random vibration: experimental results. Appl. Mech. Rev. **44**(10), 423–446 (1991)
6. Pradlwarter, H.J., Schueller, G.I.: On advanced Monte Carlo simulation procedures in stochastic structural dynamics. Int. J. Nonlinear Mech. **32**(4), 735–744 (1997)
7. Sobczyk, K., Trebicki, J.: Maximum entropy principle and nonlinear stochastic oscillators. Phys. A **193**, 448–468 (1993)
8. Ricciardi, G., Elishakoff, I.: A novel local stochastic linearization method via two extremum entropy principles. Int. J. Nonlinear Mech. **37**, 785–800 (2002)
9. Sobczyk, K., Trebicki, J.: Approximate probability distributions for stochastic systems: maximum entropy method. Comput. Methods Appl. Mech. Eng. **168**, 91–111 (1999)
10. Yong, Y., Lin, Y.K.: Exact stationary-response solution for second order nonlinear systems under parametric and external white-noise excitations. ASME J. Appl. Mech. **54**(2), 414–418 (1987)
11. Langtangen, H.P.: A general numerical solution method for Fokker-Planck equations with applications to structural reliability. Prob. Eng. Mech. **6**(1), 33–48 (1991)
12. Bergman, L.A., Masud, A.: Application of multi-scale finite element methods to the solution of the Fokker–Planck equation. Comput. Methods Appl. Mech. Eng. **194**, 1513–1526 (2005)
13. Sun, J.Q., Hsu, C.S.: The generalized cell mapping method in nonlinear random vibration based upon short-time Gaussian approximation. ASME J. Appl. Mech. **57**(4), 1018–1025 (1990)
14. Tombuyses, B., Aldemir, T.: Continuous cell-to-cell mapping. J. Sound Vib. **202**(3), 395–415 (1997)
15. Iourtchenko, D.V., Mo, E., Naess, A.: Response probability density functions of strongly nonlinear systems by the path integration method. Int. J. Nonlinear Mech. **41**, 693–705 (2006)
16. Kougioumtzoglou, I.A., Di Matteo, A., Spanos, P.D., Pirrotta, A., Di Paola, M.: An efficient Wiener path integral technique formulation for stochastic response determination of nonlinear MDOF systems. ASME J. Appl. Mech. **82**(10), 101005 (2015)
17. Psaros, A.F., Kougioumtzoglou, I.A., Petromichelakis, I.: Sparse representations and compressive sampling for enhancing the computational efficiency of the Wiener path integral technique. Mech. Syst. Signal Process. **111**, 87–101 (2018)
18. Saha, N., Roy, D.: The Girsanov linearization method for stochastically driven nonlinear oscillators. ASME J. Appl. Mech. **74**(5), 885–897 (2007)
19. Ibrahim, R.A.: Parametric Random Vibration. Research Studies Press, Letchworth (1985)
20. Assaf, S.A., Zirkie, L.D.: Approximate analysis of nonlinear stochastic systems. Int. J. Control **23**, 477–492 (1976)
21. Er, G.K.: Exponential closure method for some randomly excited non-linear systems. Int. J. Nonlinear Mech. **35**, 69–78 (2000)
22. Er, G.K.: Methodology for the solutions of some reduced Fokker-Planck equations in high dimensions. Ann. Phys. **523**(3), 247–258 (2011)
23. Er, G.K.: Probabilistic solutions of some multi-degree-of-freedom nonlinear stochastic dynamical systems excited by filtered Gaussian white noise. Comput. Phys. Commun. **185**, 1217–1222 (2014)
24. Di Paola, M., Sofi, A.: Approximated solution of the Fokker–Planck–Kolmogorov equation. Probab. Eng. Mech. **17**, 369–384 (2002)
25. Chen, L.C., Liu, J., Sun, J.Q.: Stationary response probability distribution of SDOF nonlinear stochastic systems. ASME J. Appl. Mech. **84**, 051116 (2017)
26. Martens, W., von Wagner, U., Mehrmann, V.: Calculation of high-dimensional probability density functions of stochastically excited nonlinear mechanical systems. Nonlinear Dyn. **67**, 2089–2099 (2012)
27. Bridgeman, P.W.: Dimensional Analysis. Yale University Press, New Haven (1963)
28. Zhang, S., Lin, G.: Robust data-driven discovery of governing physical laws with error bars. Proc. R. Soc. A **474**, 20180305 (2018)
29. Huang, Z.L., Tian, Y.P., Li, C.J., Lin, G., Wu, L.L., Wang, Y., Jiang, H.Q.: Data-driven automated discovery of variational laws hidden in physical systems. J. Mech. Phys. Solids **137**, 103871 (2020)
30. Lucero, J.C., Schoentgen, J.: Modeling vocal fold asymmetries with coupled van der Pol oscillators. Proc. Meet. Acoust. **19**, 060165 (2013)